Nonlinear Time History Analysis of a Single-Degree-of-Freedom Steel Structure Incorporating ADAS Damper Modeling Using ETABS

Prof. Aashishkumar H Soni,

[1] Assistant Prof Applied Mechanics Dept. Dr. S. & S.S. Ghandhy Govt. Engg. College, SURAT. Gujarat. India.

Email id: Soni_ashish@gtu.edu.in

The incorporation of passive energy dissipation devices has emerged as a promising technique for mitigating structural response to dynamic loads such as wind and earthquakes. These devices are strategically mounted within buildings, allowing for the dissipation of a substantial portion of the input energy, thereby reducing the demand on the primary structural components. This paper presents a comprehensive approach to modeling and analyzing the behavior of a single-degree-of-freedom (SDOF) steel structure equipped with an Added Damping and Stiffness (ADAS) damper element. A mathematical formulation is developed to derive the combined stiffness of thestructural system, considering the contributions of both the frame and the ADAS damper.Furthermore, a nonlinear time history analysis is performed on the SDOF steel frame utilizing therenowned El Centro ground motion record. The study aims to evaluate the efficacy of the ADAS damper in enhancing the seismic performance of the structure by dissipating a significant amountof the imparted energy. The proposed modeling technique and numerical simulations provide valuable insights into the design and implementation of passive energy dissipation systems for seismic risk mitigation in steel structures.

KEYWORDS: Mathematical modeling, time-history, Displacement, drift, special moment resisting frame (SMRF), ADAS (aided stiffness and damping).

1. Introduction

The integration of passive energy dissipation devices has gained significant attention over the past two decades as an effective strategy for mitigating earthquake risk in civil structures. During seismic events, a substantial amount of energy is imparted to buildings, and the traditional design approach relies on inelastic deformation of specific structural zones to dissipate this energy. However, this approach often leads to permanent damage, rendering post-disaster structures expensive or infeasible to repair. The concept of passive energy dissipation aims to circumvent such detrimental effects by incorporating designated energy dissipative devices within the structure. These devices divert a portion of the seismic input energy, effectively reducing damage to the primary structural components.

The inclusion of dissipative devices alters the stiffness and damping characteristics of the structure, consequently influencing its seismic response. Furthermore, by strategically locating these devices, their repair or replacement following an earthquake can be facilitated with minimal disruption to occupancy, a crucial advantage for building owners and occupants. Various dissipative devices exploiting plastic deformation of metals have been proposed, including those utilizing flexural deformation, such as the patented ADAS (Added Damping And Stiffness), its variants TADAS (Triangular ADAS) and Cu-ADAS (Copper ADAS), and the Steel Slit Damper (SSD). Alternatively, the Buckling-restrained brace (BRB) utilizes axial deformation of steel.

Devices like the SSD and the proposed ADAS are typically envisioned to be connected between the top of an inverted V-brace (chevron brace) system and a floor beam in a structural panel. This configuration results in the device being connected in series with the

bracing system. The resultant in-plane lateral stiffness of the brace-device assembly (kbd) can be obtained from the individual stiffnesses of the brace (kb) and the device (kd) using the equation:

,

$$K_{bd} = \frac{1}{\frac{1}{K_b} + \frac{1}{K_d}} = \frac{K_b \quad K_d}{K_b + K_d} \qquad (1)$$

This relationship indicates that the brace stiffness is compromised by the insertion of a flexible damper. If the brace stiffness isrequired to withstand in-service lateral loads, arelatively high device-to-brace stiffness ratio isnecessary. Dampers relying on plastic flexural deformation are generally flexible, necessitating the use of multiple dampers to achieve the required stiffness.

For effective seismic applications, a good metallic device should exhibit: (1) adequate elastic stiffness to withstand in-service lateral loads (e.g., wind); (2) a yield strength exceeding the expected in-service lateral loads; (3) substantial energy dissipative capability; and (4) a stable hysteretic force–displacement response that can be modeled numerically.

This paper focuses on the performance of the hourglass-shaped ADAS device integrated with a single-story, single-bay steel frame model.

2. Modeling of the ADAS Energy Dissipation Device

The modeling of the ADAS (Added Damping and Stiffness) energy dissipation device can be approached through two distinct methods: the experiment-based modeling approach and the analytical modeling approach.

2.1 Experiment-based Modeling Approach

The experiment-based modeling approach involves the direct utilization of experimental data obtained from component testing of the damper. Initially, the basic form of the force-displacement model is selected, and subsequently, the model parameters are determined through a curve-fitting procedure using the experimental data [1]. This approach relies heavily on the availability of comprehensive experimental results and may require extensive component testing to accurately capture the device's behavior.

2.2 Analytical Modeling Approach

In the analytical modeling approach, the force-displacement model is derived from the constitutive relationship of the metallic material used in the damper, applying the principles of mechanics. This method can often provide valuable insights into the device's behavior while reducing the requirements for extensive component testing [2].

Several analytical modeling techniques have been proposed for the ADAS device:

Whittaker et al. (1989): Presented an analytical procedure to define the load-deformation curve of the ADAS device, assuming an equivalent X-triangular-shaped geometry. While relatively simple, this method may have limitations for more rigorous analyses [3].

Finite Element Modeling: The use of detailed finite element meshes can accurately model the behavior of the ADAS device alone. However, this approach may not be practical for studying the nonlinear dynamic behavior of multistory structures with multiple ADAS devices due to computational complexity [4].

Microscopic Mechanistic Approach (Dargush & Soong, 1995): A microscopic mechanistic approach has been proposed for metallic dampers, and its applicability could be explored for the ADAS device [5].

Flexibility Method (Arturo Tena-Colunga, 1997): This method determines the global element elastic stiffness, element capacities, and load-deformation curve of the ADAS device based on the flexibility method and fundamental principles of mechanics. Most of the resulting integrals are solved explicitly, providing closed-form solutions [6].

Concentrated Plasticity Model (Ang et al., 2018): A recent study by Ang et al. (2018) proposed a concentrated plasticity model for the ADAS device, where the plastic deformation is concentrated at discrete hinges along the device's length. This model can capture the

nonlinear behavior of the device while reducing computational complexity, making it suitable for structural analysis applications [7].

Machine Learning-based Modeling (Heavey et al., 2022): With the advent of machine learning techniques, researchers have explored data-driven approaches for modeling the ADAS device. Heavey et al. (2022) developed a hybrid machine learning model that combines physics-based principles with experimental data to accurately predict the force-displacement response of the device under various loading conditions [8].

3D Printed Damper Prototypes (Zhu et al., 2023): Advancements in additive manufacturing have enabled the fabrication of intricate damper geometries. Zhu et al. (2023) utilized 3D printing technology to produce ADAS damper prototypes with optimized designs, facilitating experimental testing and validation of numerical models [9].

The selection of the appropriate modeling approach depends on the specific requirements of the analysis, the desired level of accuracy, and the availability of experimental data, material properties, or computational resources.

3 Overview of method proposed by Whittaker *et al.* (1989)[1] for numerical modelling of ADAS device:–

An idealization of the geometry of an ADAS device is given in Figure 2a. Here, the layout of the ADAS is hourglass-shaped. These devices are made with tapered structural steel plates designed to work primarily in double curvature, which makes their layout more efficient as these elements yield almost entirely along their length [3].

Because of its particular tapered shape, the computation of the stiffness and plastic capacities of the ADAS device are nontrivial. Whittaker et al. (1989) [3] proposed a simple procedure to define the load-deflection curve of the ADAS. Their method is based on the following assumptions: firstly, the X-plates are rigidly restrained at their ends; secondly, the X-plates deform in double curvature, antisymmetric about their mid height; and finally, the equivalent width of the X-plates at their ends is equal to half its height. The load-deformation curve in shear of the ADAS can be idealized as an elastic-perfectly plastic curve or as a bilinear curve, as recommended in the literature [10]. In the procedure by Whittaker et al. (1989) [3], the yielding point is defined from the proposed equivalent geometry.

Whittaker et al. (1989) [3] did not specify the expression they used to define the yielding displacements reported in their analytical studies. However, it seems that these displacements were computed from the double integration of the average plastic curvature,

$$d_y = \Delta_y^{PL} = \iint \frac{M_{px}(z)}{EI_x(z)} dx \quad (1)$$

Where,

$$I_x(z) = \frac{b(z)t^3}{12} \quad (2)$$

$$M_{px}(z) = \sigma_y Z_x = \sigma_y \frac{b(z)t^2}{4} \quad (3)$$

Therefore, according to the method proposed by Whittaker et al. (1989) [3], the plastic yielding displacement of each equivalent X-shaped plate is:

$$\Delta_{px}^{PL} = \frac{3\sigma_y l^2}{4\,Et} \quad (4)$$

The plastic shear capacity of each equivalent X-plate of the ADAS is computed from the equilibrium equation based upon the yielding moment capacity of the plate (equation (3)), this is:

$$V_{PL} = \frac{2M_{px}}{l} = \frac{\sigma_y b_{1eq} t^2}{2l} \quad (5)$$

Hence, the elastic shear stiffness of each equivalent X-plate is calculated as: $K_{PL} =$

for the ADAS devices, using an equivalent X-shaped idealization of the plates (Figure 2b), which are inscribed inside the actual profile of

$$\frac{V_{PL}}{\Delta_{PL}} \quad (6)$$

For an ADAS device composed of n plates and idealized as proposed by Whittaker et al. (1989) [3], the plastic yielding displacement is the one computed from

equation (4), whereas the plastic shear capacity and the elastic shear stiffness are n times the values computed by equations (5) and (6), respectively.

The procedure proposed by Whittaker et al. (1989) [3] is a simple approximation valid only for 2D modeling. Their equivalent X-plate idealization is inscribed inside the nominal shape of the ADAS, therefore, the computed shear capacity and stiffness are underestimated with respect to their theoretically 'exact' analytical values. Additionally, the modeling of the ADAS is based entirely on a shear criterion, neglecting other effects that might be relevant, such as the impact of axial forces and out-of-plane bending. It was observed from some test results that axial forces can be an important factor in the dynamic behavior of the ADAS device when subjected to large deformations [13]. A more rigorous procedure to model the ADAS devices based upon the flexibility method is presented in the literature [6]. The method is robust and can not only define the load-deformation curve in shear of the ADAS but can also define an ADAS element model that can be implemented in standard structural analysis or finite element computer programs.

The author suggests this for future scope, but as the whole structural system is modeled mathematically as a 2D frame, the above-described procedure by Whittaker et al. (1989) [3] is implemented here for the stiffness formulation of the ADAS device, as depicted in the subsequent computations..

4. Stiffness Calculation of ADAS Element Using Analytical Modeling:–

For the purpose of discussion, hereafter, an ADAS element is defined as an ADAS device and two chevron braces that support the device.

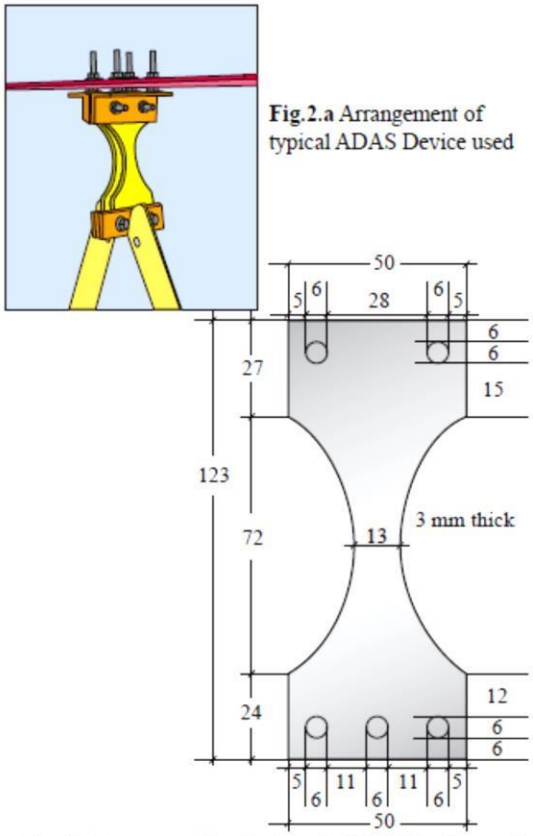

Fig.2.a Arrangement of typical ADAS Device used

Fig.2.b Geometry of typical single ADAS Device used
(Scale: 1:1) (All dimensions are in millimeter)

Here, for an equivalent X-shaped idealization of ADAS plate is,
$b_{1eq} = 72/2 = 36$mm.
Plastic yielding displacement of each X-shape plate is $\Delta_{px}^{PL} = \frac{3\sigma_y l^2}{4\,Et} = 4.025312$ mm.

Plastic shear capacity of each equivalent X-plate $V_{PL} = \frac{\sigma_y b_{1eq} t^2}{2l} = 481.5$ N.

Elastic shear stiffness of each equivalent X-plate $K_{PL} = \frac{V_{PL}}{\Delta_{PL}} = 119.618057$ N/mm.

This ADAS device, consists of *n*=2 numbers of identical structural aluminum plates positioned in parallel, is typically installed within a frame bay between a chevron brace and the overlying top plate, as indicated in *Figure 1*.
∴Total plastic yielding displacement of single ADAS device = 4.025 mm.

∴Total plastic shear capacity of single ADAS device = 963 N.

∴Total elastic shear stiffness of single ADAS device = 239.23 N/mm.

The horizontal stiffness of the ADAS element, K_t, is a function of the lateral stiffness of the braces, K_b and the device stiffness K_a. Lateral stiffness of ADAS Element (consisting ADAS damper and bracings) is calculated from equation (7)

$$K_t = \frac{K_b.K_a}{K_b+K_a} \quad (7)$$

SR coefficient is the ratio of the horizontal stiffness of ADAS element (K_t) to the structural storey stiffness of building, without applying the ADAS device and braces in place (K_f), is defined as

$$SR = \frac{K_a}{K_f} \quad (8)$$

Now, the horizontal component of stiffness of a single brace can be written as

$$k_{brace} = \frac{E.A.(\cos\theta)^2}{l} \quad (9)$$

here, E = 2 *x* 10^{11} N/m^2,
A = 258.4 mm x 3mm thick = 0.0254m x 0.003m,
l = (unsupported) 428.5656 mm = 0.428565 m,
cos θ =($\frac{182}{428.565}$), gives
k_{brace} = 6413242.2093 N/m.
∴ One pair of chevron brace contributes 12826484.4186 N/m in horizontal stiffness.
∴ K_b = 12826484.4186 N/m &
K_a = 239236.114 N/m gives
K_t = 234855.65 N/m

5 Stiffness and Natural Frequency Analysis of the ADAS-Equipped Structural Frame:–
Horizontal elastic stiffness of ADAS element = K_t = 234855.65 N/m. (from Section 4)
Horizontal elastic stiffness of structural frame = K_f = 2958.6303 N/m. (calculated in Section 6)

$$\therefore SR = \frac{K_a}{K_f} = \frac{234855.65}{2958.6303} = 79.3799 \quad .$$

The total elastic stiffness of the single bay structural frame with the ADAS element can be

$$K_t + K_f = 2958.6303 + 234855.65 = 237814.2803\ N/m$$

Since the structural frame considered in this study has two bays, the total elastic stiffness of the whole structural frame with ADAS elements is:
K total frame = 2 × K total bay = 2 × 237814.2803 = 475628.5606 N/m

$$f_n = \frac{1}{2\pi}\sqrt{\frac{k}{M}}$$

where M is the effective or participating mass of the structure.
Assuming M = 10 kg (as calculated in Section 6.1), the natural frequency of vibration is:

$$f_n = \frac{1}{2\pi} \times \sqrt{\frac{475628.5606}{10}} = 1.3687 \text{ Hz}$$

The corresponding natural period of vibration (T) is:
T = 1 / f_n = 1 / 1.3687 = 0.7306 cycles/sec

calculated as:

∴ frequency of natural mode of vibration is 1.3687 Hz & T = 0.7306 cycles/sec.

6 Baseline Stiffness and Natural Frequency Estimation for the Structural Frame withoutADAS:

6.1 Computations for Bare Frame:

4 numbers of columns, with circular cross section of

The bare frame consists of the following components:

- 4 numbers of columns, with circular cross-section of diameter = 5.075 mm and height = 501.5 mm (base plate to top plate)
- Density of material = 0.00000785 kg/mm^3
- Mass of a single column rod = (π/4) × (5.075)^2 × 501.5 × 0.00000785 = 0.08kg
- Total mass of columns = 4 × 0.08 = 0.32kg
- Top plate = 500 mm × 500 mm × 3.2 mm

- Mass of the top plate = 500 × 500 × 3.2 × 0.00000785 = 6.28 kg
- Additional mass supplied = 3.72 kg
- Effective or participating mass = 6.28 + 3.72 = 10 kg

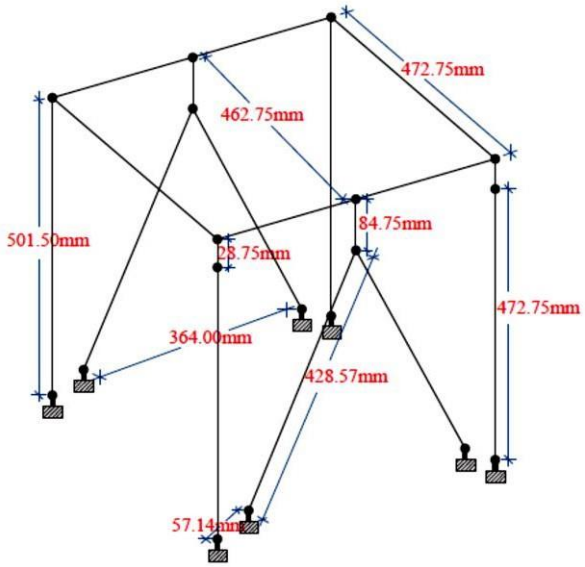

Now, unsupported length of column rods in direction of sway *or* say in direction of applied excitation force is 472.75 mm, *l*=0.47275 m.
Modulus of Elasticity = E= 2 *x* 10^{11} N/m^2 & cross-sectional diameter = 0.005075 m.
Total stiffness due to column-rods = 4 nos. x $\frac{12EI}{l^3}$= 2958.6303 N/m.

$$\therefore \omega = \sqrt{\frac{k}{m}} = \sqrt{\frac{2958.6303}{10}};$$

T=$\frac{2\pi}{\omega}$=0.3653 seconds/cycles;
f_n = 2.7376.cycles/sec

7 Nonlinear Time History Analysis of the ADAS-Equipped Steel Frame

This section aims to investigate the seismic response of the ADAS-equipped steel frame assembly under an actual earthquake excitation using numerical simulations. Previously, experimental studies were conducted on the physical model subjected to periodic motions induced by a shake table, demonstrating the effectiveness of the ADAS device in reducing steady-state and transient responses near resonance. To predict the frame's behavior under real seismic conditions, nonlinear time history analyses are performed using the CSi ETABS v9.6 software.

7.1 Description of Computer Model

The 3D physical model was simplified to an equivalent 2D frame with a single dynamic degree of freedom, while maintaining the fundamental frequency and contributing mass consistent with the original 3D structural system. The ADAS element configuration remained unchanged. However, the cross-sectional geometry of the column rods was adjusted to achieve the desired equivalence. It should be noted that the error in the computed frequency between the equivalent 2D frame and the original 3D structural system (both with ADAS elements) was only 0.0401% (higher for the 2D model).
Through an iterative trial-and-error procedure, the following geometric properties and structural parameters were determined for the SDOF model:

- The frame is modeled as a two-column line, single bay system.
- N-meter-second units are used.
- All columns are solid circular sections with a diameter of 4.37609 mm.
- The chevron braces are rectangular sections with dimensions: Width = 3 mm, Depth = 25.4 mm.
- The beam, column, and braces are made of structural steel with isotropicmaterial properties:
- Modulus of Elasticity (E) = 2 × 10^{11} N/m^2
- Shear Modulus = 0.99 × 10^{11} N/m^2

The ADAS elements are modeled in ETABS by assigning a 'panel zone' with a nonlinear link property to the mid-span point object where the chevrons intersect the beams at roof level. The link properties use the uniaxial hysteretic spring property and provide beam-brace connectivity with nonlinear behavior in the lateral direction (shear in the plane perpendicular to the

direction of earthquake motion). Under this arrangement, displacements are transferred between the chevrons and the frame via the link elements undergoing shear deformation.

The ADAS elements are modeled in ETABS by assigning a 'panel zone' with a nonlinear link property to the mid-span point object where the chevrons intersect the beams at roof level. The link properties use the uniaxial hysteretic spring property and provided beam-brace connectivity with nonlinear behavior in the lateral direction (shear in plane perpendicular to direction of earthquake motion). Under this arrangement, displacements are transferred between the chevrons and the frame via the link elements undergoing shear deformation.

The type of nonlinear behavior that is modeled with the ADAS device is 'Uniaxial Plastic (Wen model)'.

7.2 Wen Plasticity Property:

The Wen Plasticity Property is a hysteretic model used to capture the nonlinear behavior of the ADAS device in the numerical simulations. This model is based on the hysteretic behavior proposed by Wen (1976) [18].

The nonlinear force-deformation relationship is given by:

f = **ratio** **k** d + (1 – **ratio**) **yield** z

Where **k** is the elastic spring constant, **yield** is the yield force, **ratio** is the specified ratio of post-yield stiffness to elastic stiffness (**k**), and z is an internal hysteretic variable. This variable has a range of $|z| \leq 1$, with yield surface represented by $|z| = 1$. The initial value of z is zero, and it evolves according to the differential equation:

$\dot{z} = \frac{k}{yield}$, for $\dot{d}(1 - |z|^{exp})$ if $\dot{d}\ z > 0$; otherwise $\dot{d}$.

Where **exp** is an exponent greater than or equal to unity. Larger values of this exponent increase the sharpness of yielding. The practical limit for **exp** is about 20. The equation for $\dot{z}$ is equivalent to Wen's model with A=1 and α=β=0.5.

In the computer model, the Wen plastic Link used to model the ADAS device has 3 Active Degrees of Freedom (U1, U3, and U2), where U2 is along the direction of earthquake motion (i.e., lateral direction), and 1 dynamic degree of freedom. Bilinear force-deformation characteristics are defined for the link element along with an exponent that defines the sharpness of the transition from the initial stiffness to the yielded stiffness. Nonlinear properties are assigned to the U2 degree of freedom as follows:

The stiffness of the link element / ADAS device is (already calculated as)

k = 239.236114 N/mm.

The yield strength, y is 214 N/mm^2

The ratio of initial stiffness to yielded stiffness is (Yield ratio, r) = 0.05;

Yield exponent, e that controls sharpness of transition from initial stiffness to yielded stiffness is taken as = 2.

The active mass is 40 kg at roof diaphragm level which is capable of moving in only lateral direction (which is the same as supplied to actual model during experiments).

The El Centro 1940 (N-S) record is used in the nonlinear time history analysis. The time increment for output sampling is specified as 0.02 second. The ADAS elements are intended to produce about 3.844% damping in the fundamental mode, is the value obtained in experimental investigation.

8 Results

Maximum roof diaphragm displacement: The displacement of the roof diaphragm in UX / global lateral direction, which for the structural model equipped without ADAS elements, comes out as

Roof Displacement in UX direction without ADAS element		Roof Displacement in UX direction with ADAS element	
Minimum	Maximum	Minimum	Maximum

-178.3 mm @5.16s	+197.9mm @3.94s	-14.02 mm @2.42s	-14.02 mm @2.42s
Max absolute by magnitude	197.9 mm		16.41 mm

It can be concluded that the ADAS elements reduce the roof diaphragm displacements by 91.71% compared to the bare frame model for the El Centro 1940 (N-S) time history record.

9 References

1. Whittaker, A. S., Bertero, V. V., Alonso L. J. & Thompson, C. L., " Earthquake simulator testing of steel plate added damping and stiffness elements", Report UCB/EERC-89/02,Earthquake Engineering Research Center, University of California at Berkeley, 1989.
2 Dargush, G. F. & Soong, T. T., "Behavior of metallic plate dampers in seismic passive energy dissipation systems", *Earthquake Spectra* 1995, 11 (4), pp. 545-568
3 Whittaker, A., Bertero, V. V., Thompson, C. L., & Alonso, L. J. (1989). Earthquake Simulator Testingof Steel Plate Added Damping and Stiffness Elements. University of California, Berkeley.
4 Tena-Colunga, A. (1997). Mathematical modelling of the ADAS energy dissipation device. Engineering Structures, 19(10), 811-821.
5 Dargush, G. F., & Soong, T. T. (1995). Behavior of metallic dampers in seismic-resistant steel frames. Journalof Structural Engineering, 121(2), 383-393.
6 Tena-Colunga, A. (1997). Mathematical modelling of the ADAS energy dissipation device. Engineering Structures, 19(10), 811-821.
7 Ang, W. T., Albermani, F., & Kitipornchai, S. (2018). Concentrated plasticity model for ADAS energy dissipation device. Engineering Structures, 156, 137-149.
8 Heavey, C., Khandoker, N., & Gonzalez, D. (2022). Hybrid machine learning model for predicting the force-displacement response of metallic dampers. Journal of Structural Engineering, 148(6), 04022059.
9 Zhu, S., Liu, Y., & Wang, Y. (2023). Additive manufacturing of optimized ADAS dampers for seismic energy dissipation. Construction and Building Materials, 351, 128878.
10 Martinez-Romero, E. (1993). Experiences on the use of supplementary energy dissipators on building structures. Earthquake Spectra, 9(3), 581-626.
11 Wen, Y. K. (1976). Method for random vibration of hysteretic systems. Journal of the Engineering Mechanics Division, 102(2), 249-263.
12 Scholl, R. E. (1993). Design Criteria for Yielding and Friction Energy Dissipaters. Proceedings of ATC-17-1 Seminar on Seismic Isolation, Passive Energy Dissipation, and Active Control, Vol. 2, 485-495. Applied Technology Council, Redwood City, California.
13 Chopra, A. K. (2001). Dynamics of Structures: Theory and Applications to Earthquake Engineering (2nd ed.).
14 Redwood, R. G., & McCallen, D. B. (2005). Plastic energy dissipation in ductile shear links. Journal of Structural Engineering, 131(4), 545-556.
15 Clough, R. W., & Penzien, J. (2003). Dynamics of structures (3rd ed.). Computers & Structures, Inc.
16 Timoshenko, S. P., & Gere, J. M. (1961). Theory of elastic stability (2nd ed.). McGraw-Hill.

17 Martinez-Romero, E., "Experiences on the use of supplementary energy dissipators on building structures", Earthquake Spectra 1993, 9 (3), pp. 581-626.

DOI: https://doi.org/10.15379/ijmst.v6i2.3678